Regulation of Class IA PI 3-kinases: C2 domain-iSH2 domain contacts inhibit p85/p110α and are disrupted in oncogenic p85 mutants

Haiyan Wu[a], S. Chandra Shekar[a], Rory J. Flinn[a], Mirvat El-Sibai[b], Bijay S. Jaiswal[c], K. Ilker Sen[d], Vasantharajan Janakiraman[c], Somasekar Seshagiri[c], Gary J. Gerfen[d], Mark E. Girvin[e], and Jonathan M. Backer[a,1]

[a]Departments of Molecular Pharmacology, [d]Physiology and Biophysics, and [e]Biochemistry, Albert Einstein College of Medicine, 1300 Morris Park Avenue, Bronx, NY, 10461; [b]Department of Natural Sciences, Lebanese American University, Beirut Campus, Beirut, Lebanon; and [c]Department of Molecular Biology, Genetech Inc., 1 DNA Way, South San Francisco, CA 94080

Edited by Peter K. Vogt, Scripps Research Institute, La Jolla, CA, and approved October 7, 2009 (received for review March 3, 2009)

We previously proposed a model of Class IA PI3K regulation in which p85 inhibition of p110α requires (*i*) an inhibitory contact between the p85 nSH2 domain and the p110α helical domain, and (*ii*) a contact between the p85 nSH2 and iSH2 domains that orients the nSH2 so as to inhibit p110α. We proposed that oncogenic truncations of p85 fail to inhibit p110 due to a loss of the iSH2-nSH2 contact. However, we now find that within the context of a minimal regulatory fragment of p85 (the nSH2-iSH2 fragment, termed p85ni), the nSH2 domain rotates much more freely ($\tau_c \approx$12.7 ns) than it could if it were interacting rigidly with the iSH2 domain. These data are not compatible with our previous model. We therefore tested an alternative model in which oncogenic p85 truncations destabilize an interface between the p110α C2 domain (residue N345) and the p85 iSH2 domain (residues D560 and N564). p85ni-D560K/N564K shows reduced inhibition of p110α, similar to the truncated p85ni-572^{STOP}. Conversely, wild-type p85ni poorly inhibits p110αN345K. Strikingly, the p110αN345K mutant is inhibited to the same extent by the wild-type or truncated p85ni, suggesting that mutation of p110α-N345 is not additive with the p85ni-572^{STOP} mutation. Similarly, the D560K/N564K mutation is not additive with the p85ni-572^{STOP} mutant for downstream signaling or cellular transformation. Thus, our data suggests that mutations at the C2-iSH2 domain contact and truncations of the iSH2 domain, which are found in human tumors, both act by disrupting the C2-iSH2 domain interface.

cancer | glioblastoma | phosphoinositide 3-kinase | PIK3CA

PI 3-kinases are important cellular regulators of growth, survival, and motility, and deregulation of PI 3-kinase signaling contributes to cancer and other human diseases (1). Class IA PI 3-kinases, which produce PI[3,4,5]P3 in intact cells (2), are obligate heterodimers of a regulatory subunit (p85α, p85β, p55α, p50α, or p55γ) and a catalytic subunit (p110α, p110β, or p110δ) (reviewed in ref. 3). The regulatory subunits have two major functions: they stabilize the catalytic subunits against thermal denaturation, and they maintain the catalytic subunit in an inhibited, low activity state (4, 5).

p85 and p110 are both multidomain proteins that bind to each other and to upstream activators such as Rac and Cdc42, Ras, and tyrosine phosphorylated receptors and adapters (reviewed in ref. 6). p85 contains an SH3 domain, a Rac/Cdc42-binding domain homologous to a GAP domain in the BCR gene product, and two SH2 domains that flank an antiparallel coiled coil domain (the iSH2 domain). While NMR, EPR, and crystal structures have been obtained for the individual domains (7–15), there are currently no structures that define how these domains are arranged in space. The p110α catalytic subunit has been better defined, with structures of the N-terminal adapter-binding domain (ABD) or the entire p110α bound to the coiled coil (iSH2) domain of p85 (15, 16). Like the related Class IB catalytic subunit p110γ (17), p110α contains Ras-binding, C2, helical, and kinase domains. In the p110α structure, p110α is anchored by the binding of the N-terminal ABD to the far end of the rod-like iSH2 domain, consistent with previous biochemical studies (18–20). The kinase and C2 domains drape over the iSH2 domain like a saddle, with the Ras-binding domain facing upward above the ABD. The helical domain is positioned at the opposite end of the molecule from the ABD, and is therefore close to the ends of the iSH2 domain that are linked to the two SH2 domains.

Structural studies on p110γ and p110α have not provided a mechanism to explain the inhibition of p110α by p85 binding, or the activation of p85/p110α dimers by phosphoprotein binding to the SH2 domains of p85 (21, 22). We and others have shown that the iSH2 domain-ABD interface is structurally rigid and does not regulate p110 activity (23–25). In contrast, the N-terminal SH2 (nSH2) domain of p85 is required for inhibition of p110α. Recent biochemical studies suggest that basic residues surrounding the phosphopeptide binding site in the nSH2 domain make an inhibitory contact with an acidic patch in the helical domain of p110α (15). Phosphoprotein binding to the SH2 domain would presumably disrupt this inhibitory contact and activate the p85/p110 dimer. This interface is also disrupted by oncogenic mutations in the helical domain of p110 that have been identified in human cancers (15, 26). Helical domain mutations in p110α synergize with activated Ras for activation of PI 3-kinase (27).

Oncogenic mutations have been described in p85, mostly truncations or deletions in the C-terminal end of the iSH2 domain (28–30); more recent sequencing studies have identified additional deletion and point mutations in the iSH2 domain (31, 32). The oncogenic p85 mutations presumably act by disrupting inhibitory contacts with p110α, and the p85572^{STOP} and p85 (Δ583–605) mutants (28, 30) fail to inhibit p110α in vitro (33). We previously examined the structure of the minimal regulatory portion of p85, the nSH2-iSH2 fragment (p85ni) (23). Based on NMR experiments that measured the relaxation of nSH2 domain amide protons by spin probes in the iSH2 domain within p85ni, we proposed that contacts between the C-terminal end of the iSH2 domain and the nSH2 domain position the latter domain such that it forms an inhibitory contact with p110α (33). Loss of these contacts in the oncogenic p85 mutants would explain the loss of p110α inhibition. However, several recent data have led

Author contributions: K.I.S., G.J.G., M.E.G., and J.M.B. designed research; H.W., S.C.S., R.J.F., M.E.-S., and B.S.J. performed research; V.J. and S.S. contributed new reagents/analytic tools; H.W., S.C.S., M.E.-S., K.I.S., G.J.G., M.E.G., and J.M.B. analyzed data; and M.E.G. and J.M.B. wrote the paper.

The authors declare no conflict of interest.

This article is a PNAS Direct Submission.

[1]To whom correspondence should be addressed. E-mail: backer@aecom.yu.edu.

This article contains supporting information online at www.pnas.org/cgi/content/full/0902369106/DCSupplemental.

us to revisit our original hypothesis. First of all, analysis of the relative positions of the nSH2 and iSH2 domains within p85ni by pulsed EPR spectroscopy in frozen solution suggest the presence of significant disorder between the nSH2 and iSH2 domains (K. I. Sen and G. J. Gerfen, unpublished observations). Furthermore, the identification of contacts between the C2 domain of p110α and residues around 560–564 in the iSH2 domain led to an alternative model, in which truncation at 572 would destabilize C2-iSH2 domain contacts that are required for inhibition of p110α (16, 32).

In light of the structural data on p110α, we have used biophysical and biochemical approaches to revisit the mechanism by which mutations in the iSH2 domain lead to a loss of p110α inhibition. Contrary to our previous interpretation, measurement of the rotational freedom of the nSH2 domain within p85ni suggest that the nSH2 domain is not rigidly constrained by interactions with the iSH2 domain, and is therefore unlikely to adopt a fixed orientation with p85ni. In contrast, mutations that specifically disrupt the C2-iSH2 domain contact led to a loss of p110α inhibition, and are redundant with oncogenic p85 truncation mutants with respect to effects on p110α activity in vitro and signaling and transformation in vivo. Our data support a model in which oncogenic p85 mutations lead to a loss of a C2-iSH2 domain contact that is required for inhibition of p110α by p85.

Results

NMR Analysis of nSH2 Dynamics. We previously analyzed the relative orientation of the nSH2 and iSH2 domains within the minimal regulatory fragment of p85, the nSH2-iSH2 fragment (p85ni), using NMR paramagnetic relaxation methods. Spin probes in the iSH2 domain were used to perturb the NMR signals from assigned residues in the nSH2 domain (33). The strong relaxation effects observed for a limited set of residues, which were confined to a single face of the nSH2 domain, implied a defined interface between the two domains. However, because of the strong distance-dependence of these paramagnetic relaxation effects (varying with distance to the sixth power), a more transient interaction with a preferred contact orientation could also be consistent with the measured effects. To distinguish between these two possibilities, we used ^{15}N NMR relaxation methods to measure the rotational dynamics of the nSH2 domain within the p85ni construct.

TROSY-based ^{15}N relaxation data were collected on uniformly ^{2}H^{15}N-labeled p85ni. Since the signals from the residues in the long coiled-coil have steadfastly resisted NMR assignment methods, we focused on the properties of the resonances from the nSH2 domain. For the 73 resonances that we have assigned in the SH2 domain (28), 49 appeared to be sufficiently ordered ($\{^{1}$H$\}^{15}$N NOE/noNOE >0.75), and uninvolved in intermediate exchange processes (having representative R_2/R_1 ratios) to reliably report on the overall rotational motion of the SH2 domain. The R_2/R_1 ratios for the cross peaks of these residues (Fig. S1), defined an apparent rotational correlation time of 12.7 $\pm$ 0.7 ns for the nSH2 domain. Hydrodynamics calculations (34) for the individual nSH2 domain, iSH2 domain, and several proposed p85ni geometries yield predicted rotational correlation times of 8.5, 27.5, and 45–52 ns, respectively, and experimental measurements for isolated SH2 domains range from 6.5 to 9.2 ns (34–37). Hence while the rotation of the nSH2 domain is partially restricted by its tether to the iSH2 domain, it appears to be quite mobile with respect to the long iSH2 coiled-coil. These data are not compatible with our previous model of how truncations in the distal iSH2 domain lead to a loss of p110α inhibition.

Role of C2 Domain-iSH2 Domain Contacts in the Inhibition of p110α. We next tested the alternative model proposed by Huang et al. (16), in which iSH2 truncations destabilize p85/p110 contacts involving the C2 domain of p110α (at residue N345) and the iSH2 domain of p85 (at residues D560 and N564). Wild-type p110α was inhibited 80% by wild-type p85ni, but was inhibited only 40% by a p85ni-D560K/N564K mutant (Fig. 1*B*), which bound normally to p110α (Fig. 1*A*, *Top*). Importantly, inhibition by p85ni-D560K/N564K was not statistically different from that seen with the p85ni572^{stop} truncation mutant. Similarly, mutation of the p110α contact site (p110αN345K) had no effect of binding to p85ni (Fig. 1*A*, *Bottom*) but led to a loss of inhibition by wild-type p85ni (from 80% inhibition to 40%) (Fig. 1*B*). Sequencing data has recently identified mutations of p110α residues N345 and p85α residues D560 and N564 in human cancers (26, 31, 32); our data suggests that mutations of these residues should lead to constitutive increases in PI 3-kinase activity.

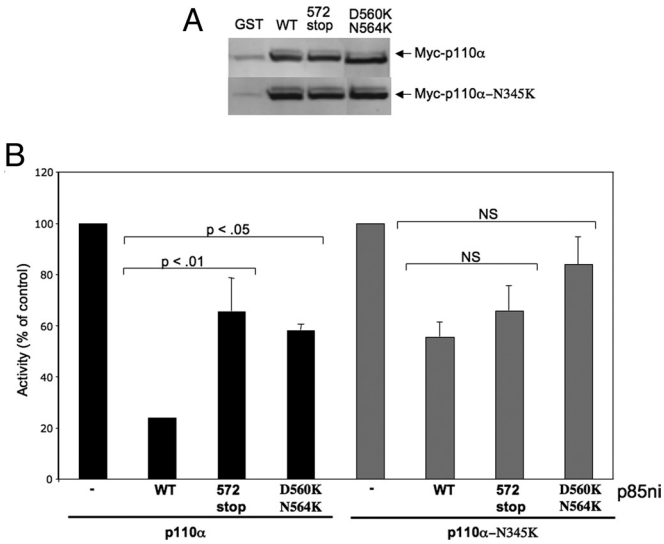

Fig. 1. Disruption of C2-iSH2 domain contacts is redundant with oncogenic truncation of p85ni. (*A*) Two micrograms of purified GST or wild-type or mutant GST-p85ni was immobilized on glutathione-Sepharose beads, and incubated with lysates from HEK293T cells transfected with myc-p110α or myc-p110αN345K. The beads were washed and bound proteins were blotted with anti-myc antibody. (*B*) Recombinant wild-type or mutant p110α was incubated for 1 h at 4 °C without or with wild-type or mutant p85ni and assayed for lipid activity at 22 °C as described. The data are the mean $\pm$ SEM of triplicate determinations from three experiments.

While mutation of D560/N564 mimics the effect of the p85ni572^{stop} truncation, this does not mean that the phenotypes of the two mutations are mechanistically related. To test this directly, we reasoned that if the effect of the p85ni572^{stop} mutation was due to a disruption of the iSH2-C2 domain contact, then a p110 mutant in which the contact had already been disrupted (p110αN345K) would not be able to discriminate between full-length and truncated p85ni; inhibition of such a mutant should be the same for both constructs. This predicted result was in fact observed: whereas the inhibition of wild-type p110α by p85ni vs. p85ni571^{stop} differed by >2-fold (80% vs. 35% inhibition) (Fig. 1*B*, *Left*), the inhibition of p110αN345K by the two p85ni constructs was showed no statistically significant difference (Fig. 1*C*, *Right*).

p85 Truncations and Mutations of the iSH2-C2 Contact Are Not Additive for Activation of Downstream Signaling. As an independent measure of whether the p85ni572^{STOP} mutant is mechanistically linked to the mutants at the C2-iSH2 domain interface, we tested whether the mutations caused additive activation of PI 3-kinase in vivo. In transient transfections in HEK293T cells, expression of p85ni571^{STOP}, p85niD560K/N564K and a double mutant,

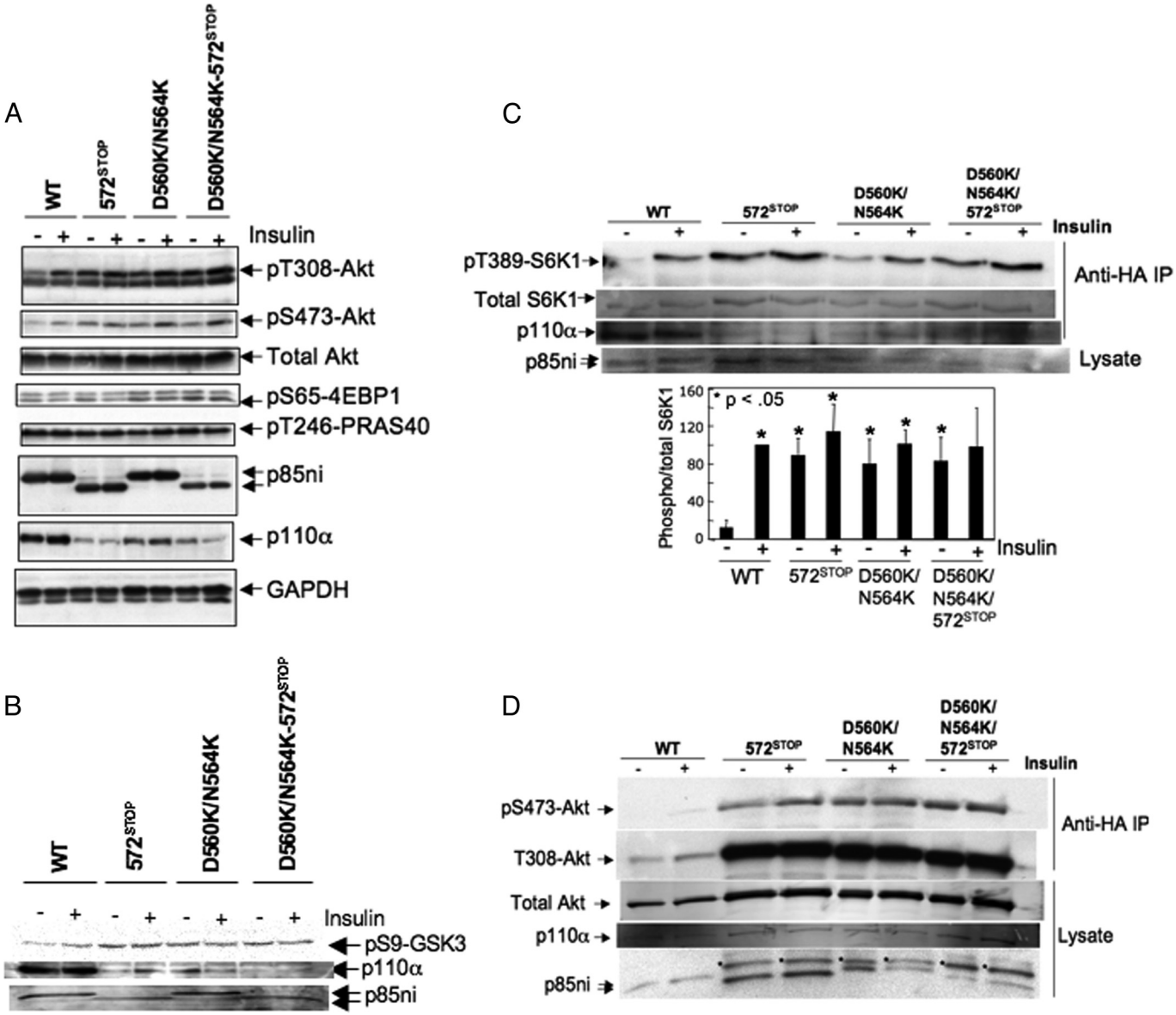

Fig. 2. Truncation mutants and C2-iSH2 contact mutants of p85 are redundant for activation of downstream signaling. (*A*) HEK293T cells were transiently transfected with myc-p110α and wild-type or mutant p85ni. Cells were incubated without or with insulin, lysed, and blotted for p85 and p110α, for total and phosphorylated forms of Akt, and for phosphorylated 4EBP1, and PRAS40 as shown. The data are representative of five separate experiments (*B*) Cells were transfected and stimulated as above and blotted for pSer9-GSK3, p85ni and p110α. The data are representative of three separate experiments. (*C*) HEK293E cells were transiently transfected with HA-S6K1, myc-p110α and wild-type or mutant p85ni. Anti-HA immunoprecipitates were blotted for total and phosphorylated S6K1 and for myc-p110α (which binds to HA-p85ni). Lysates were blotted for p85ni. The ratio of pT389/total S6K1 was determined using a LICOR Odyssey imaging system, and is the mean $\pm$ SD from three experiments. (*D*) HEK293T cells were transiently transfected with HA-Akt, myc-p110α and wild-type or mutant HA-p85ni. Anti-HA immunoprecipitates were blotted for total and phosphorylated Akt and for myc-p110α (which binds to HA-p85ni). Lysates were blotted for p85ni. The data are representative of two separate experiments.

p85niD560K/N564K/572^{STOP}, caused similar increases in both basal and insulin stimulated activation of endogenous Akt (measured by phosphorylation at T308 and S473) (Fig. 2*A*). Phosphorylation of PRAS40 at T246 was unaffected by the mutations, whereas phosphorylation of 4EBP1 at S65 was increased under basal conditions in cells expressing the p85ni mutants (Fig. 2*A*), as was phosphorylation of GSK3 (Fig. 2*B*). We also produced stably transfected Baf3 cells, and found that although the basal activation of Akt was higher in cells expressing p85ni571STOP as opposed to p85niD560K/N564K, no additively was seen with the double mutant (Fig. S2*A*). We were unable to clearly detect changes in endogenous S6K1 in whole cell lysates, so we co-transfected cells with wild-type or mutant p85ni and HA-tagged S6K1. Phosphorylation of S6K1 at T389 was somewhat higher in cells expressing p85ni571^{STOP} as opposed to p85niD560K/N564K, but once again no additively was seen with the double mutant (Fig. 2*C*, top); this is more evident when the ratio of phosphorylated to total S6K1 is calculated (Fig. 2*C*, lower panel). Co-transfection of wild-type or mutant p85ni with HA-Akt led to similar increases in phosphorylation of S473 with all of the mutants as compared to cells expressing wild-type p85ni (Fig. 2*D*). These data show that deletion of p85ni after residue 571, or mutation of the C2/iSH2 domain interface, have similar effects on downstream signaling.

We compared the ability of wild-type and mutant p85ni to bind to activated PDGF receptors at the plasma membrane. Both

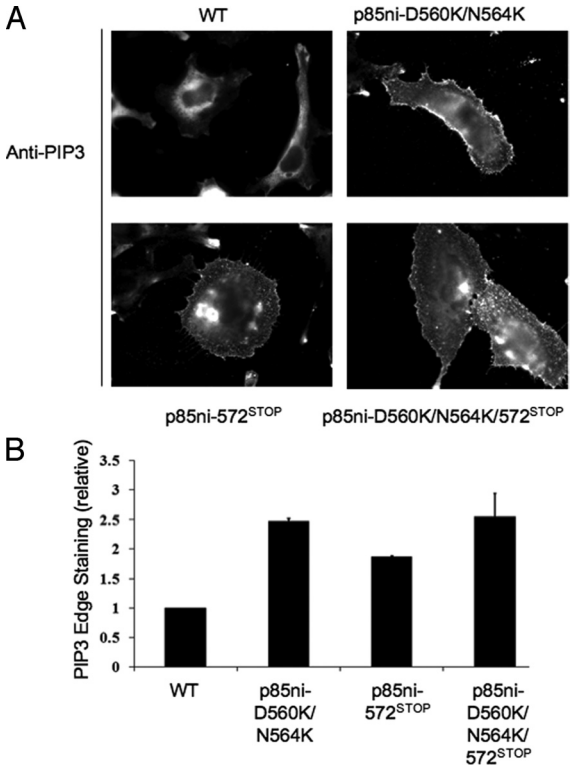

Fig. 3. Effects of truncation mutants and C2-iSH2 contact mutants of p85 on PIP3 production in vivo. HeLa cells were transfected with myc-p110α and wild-type or mutant p85ni. The cells were rendered quiescent overnight, fixed, and stained with anti-PIP3 antibody. Cells were imaged using a Nikon 60 $\times$ 1.4 NA objective and a Roper cooled-CCD camera. Quantitation of PIP3 was performed as described in ref. 44. The data are the mean $\pm$ SD from two independent experiments.

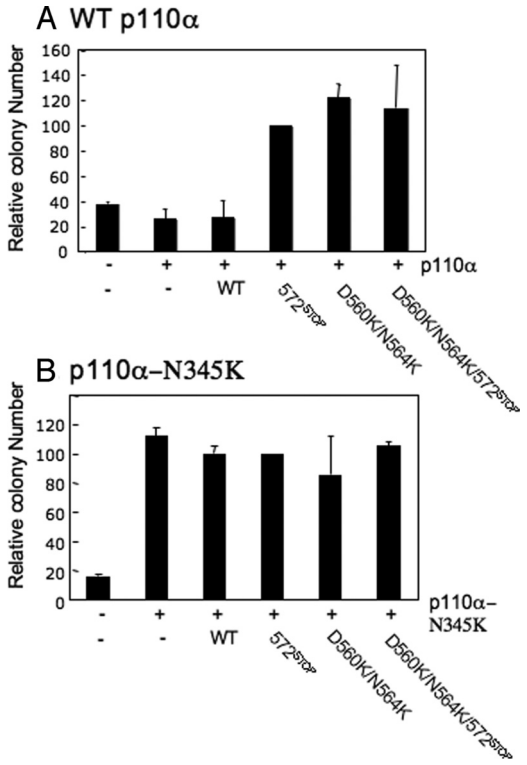

Fig. 4. Effects of truncation mutants and C2-iSH2 contact mutants of p85 on transformation. (*A*) NIH 3T3 cells were transiently transfected with myc-p110α and wild-type or mutant p85ni. The cells were plated in soft agar as described and colonies were counted after 3 weeks. Colony counts were normalized to the number produced by cells expressing p85ni572^{STOP}. The data are the mean $\pm$ SEM from three experiments. (*B*) NIH 3T3 cells were transiently transfected with p110α-N345K and wild-type or mutant p85ni. Colony counts were normalized to the number produced by cells expressing p85ni572^{STOP}. The data are the mean $\pm$ SD from 2–3 experiments.

wild-type and mutant p85ni showed similar binding, as would be expected for an SH2-mediated process (Fig. S2*B*). To evaluate the effects on intracellular PIP3 production, we stained quiescent cells expressing wild-type or mutant p85ni and stained cells with an anti-PIP3 antibody that we have previously characterized (38). Quiescent cells expressing mutant p85ni showed increased PIP3 production at the cell edge as compared to cells expressing wild-type p85ni, and no additively between the truncation and C2/iSH2 interface mutants was seen (Fig. 3 *A* and *B*). Unlike PIP3 staining at the cell periphery, the diffuse staining in the center of the cell is nonspecific, as it has been previously be shown to be resistant to wortmannin (38).

Finally, we measured transformation in NIH 3T3 cells co-transfected with wild-type or N345K p110α, and wild-type or mutant p85ni, using a soft agar growth assay. Minimal colony formation was found in cells expressing p110α and wild-type p85, whereas cells expressing p85ni571^{STOP}, p85niD560K/N564K, or p85niD560K/N564K/572^{STOP} showed similar $\approx$4-fold increases in colony number (Fig. 4*A*). Cells expressing p110α-N345K showed an $\approx$5-fold increase in colony formation, and no additional increase in transformation was seen in cells co-transfected with mutant p85ni (Fig. 4*B*). Taken together, these biochemical data fail to show additivity between the two types of p85 mutant, or between the C2-domain p110α mutant and iSH2 domain mutants of p85. These data suggest that these mutations all exert their effect on p110α activity by disruption of the inhibitory C2-iSH2 domain interface.

Discussion

We have previously shown that inhibition of p110α by p85 requires a charge-based interaction between the nSH2 domain of p85 and the helical domain of p110α (15). We now show that a second interaction, involving the residues D560 and N564 of the iSH2 domain and residue N345 in the C2 domain of p110, is also required for inhibition of p110α. Disruption of this second interface leads to a loss of inhibition in vitro, and constitutive activation of Akt in transfected cells. The importance of the C2-iSH2 domain interface was first predicted based on the crystal structure of the p110α/iSH2 dimer (16), and sequencing studies have identified mutations at p110αN345, as well as p85α D560 and N564, in human cancers (26, 31, 32). Mutational disruption of the C2-iSH2 domain interface is likely to lead to constitutive activation of Class IA PI 3-kinase in vivo and contribute to tumorigenesis, and we find that mutations in p85ni or p110α that disrupt this interface lead to constitutive increases in downstream signaling as well as increased rates of transformation. A previous study showed that the p110α-N345K mutant had strong transforming potential, but was less potent than the hotspot mutations (E545K and H1047R) (39). Based on our mechanistic data, one would expect a similar potency for the iSH2 mutants, although their ability to interact with p110β and p110δ could increase their tumorigenicity in vivo even more.

A second aspect of this study examines the mechanism by which oncogenic mutations in the C-terminal end of the iSH2 domain (28–30) lead to PI 3-kinase activation. We previously proposed that oncogenic truncations of p85 remove nSH2-iSH2 domain contacts that orient the nSH2 domain so as to inhibit p110α (33). This hypothesis was based on the finding that spin probes in the iSH2 domain produced significant relaxation

effects on NMR crosspeaks from residues in one face of the nSH2 domain, which we interpreted as showing a preferred orientation of the nSH2 domain relative to the iSH2 domain. However, based on the NMR data present in this paper, we think it more likely that within the context of p85ni, the nSH2 domain moves rapidly with respect to the iSH2 domain, with a rotational correlation time on the order of 13 ns. These data make it unlikely that the nSH2 domain is constrained by interactions with the iSH2 domain. In a related study, a pulsed EPR analysis of the relative positions of the nSH2 and iSH2 domains within p85ni strongly suggest that the nSH2 domain is not rigidly fixed (K. I. Sen and G. J. Gerfen, unpublished observations). Interestingly, the EPR data suggest that the motion of the nSH2 domain is not random, but is restrained to a torus-like distribution around the proximal end of the iSH2 domain. Thus, the nSH2 domain moves in a hinge-like manner, and not like a ball on a string. This restricted motion presumably explains why relaxation effects from iSH2 spin labels were only seen on one face of the nSH2 domain in our earlier study (33). Preliminary data suggest that the nSH2 domain is also mobile in the context of intact p85; studies to evaluate the relative mobility of the nSH2 domain in p85/p110 dimers are currently being pursued.

With regard to oncogenic truncation mutants of p85, our mutagenesis data strongly support an alternative hypothesis, originally proposed by Huang et al. (16) and elaborated in a recent study of mutations in glioblastoma (32). These two studies suggest that truncation of p85 after residue 571 might destabilize a contact between the iSH2 domain and the C2 domain of p110α. Consistent with this hypothesis, we find that mutation of p85ni D560 and N564 to Lys mimics the effects of truncation after p85 residue 571, and inhibition of p110αN345K by wild-type or truncated p85ni is similar. Furthermore, the effects of mutation at p85ni-D560/N564 and truncation after residue 571 lead to similar levels of constitutive PI 3-kinase-dependent signaling in vivo and similar levels of transformation. While there is some variability between different downstream enzymes as to whether the D560/N564 mutant or the 572^{STOP} mutant has the larger effect, in no cases are the mutations additive. Our data thus support the hypothesis that iSH2 domain truncations destabilize iSH2-C2 domain contacts (16, 32).

It should be noted that the mobility of the nSH2 in the context of p85ni, or even intact p85, might not reflect its motion within the p85/p110 dimers. However, the ability of the nSH2 domain to move is in fact consistent with our previous model of p85/p110 regulation by nSH2 domain occupancy (15). Given that the nSH2 phosphopeptide binding site contacts the E542/E545 acidic patch in the helical domain of p110α, the nSH2 domain must move away from the helical domain to accommodate the binding of tyrosine phosphorylated activators. Biochemical data in fact suggest that the ability of nSH2 domain to move about the proximal end of the iSH2 domain is necessary for PI 3-kinase activation, as introduction of an engineered disulfide bond between the nSH2 and iSH2 domains produces a mutant than inhibits p110, but cannot be activated by phosphopeptides.

Our data demonstrate the in addition to the inhibitory nSH2-helical domain interface, a second interface involving the iSH2 domain and the p110α C2 domain is also inhibitory. While our data show that recently identified mutations at the iSH2-C2 interface (31, 32) lead to increased PI 3-kinase signaling, it is not yet known whether this interface is regulated in wild-type p110α. It also remains to be seen whether the inhibitory interfaces involving the C2 and helical domains of p110α are mechanistically related. Given that the primary tethering site between p110 and p85 involves the iSH2 domain and the N-terminal ABD of p110α, a second stabilizing contact between the C2 and iSH2 domains may be required for the proper alignment of the helical domain-nSH2 domain interface, which is the site of phosphopeptide regulation of p85/p110. Alternatively, the C2-iSH2 domain contact may directly affect the conformation of the kinase domain. If so, it will be interesting to see if known activators of p85/p110α, such as Rac/CDC42, Ras, and tyrosine phosphoproteins (6), cause changes in the intersubunit contacts at C2-iSH2 domain interface. Finally, it is worth noting that the identification of regulated inhibitory interfaces between p85 and p110 could facilitate the development of pharmacological compounds that inhibit PI 3-kinases by stabilizing these interfaces, rather than by blocking the ATP-binding site.

Experimental Procedures

Protein Expression and Purification. Uniformly ^{15}N-labeled recombinant human p85ni (residues 321–600) was produced as a GST fusion in bacteria grown in minimal medium supplemented with $^{15}NH_4Cl$, and harvested by thrombin cleavage of glutathione-Sepharose-bound material. The final sample was ≈1 mM protein in PBS, pH 7.4, containing 0.5% Nonidet P-40. Mutants of bovine p110α or p85ni were produced using 4-primer PCR methods. All constructs were confirmed by sequencing. Wild-type and mutant p110α was produced in baculovirus-infected Sf-9 cells. Wild-type and mutant p85ni were produced as above.

NMR Spectroscopy. All NMR relaxation data were acquired at 28 °C on a cryoprobe-equipped Bruker 800 MHz spectrometer at the New York Structural Biology Center, using TROSY-based pulse sequences adapted from those described by Zhu et al. (40). All sequences were modified to maintain water magnetization along Z throughout the experiment by using selective flip-back water 90° pulses and selectively nonexciting 180° pulses via a watergate 3–9-19 motif. All three pulse sequences used TROSY component selection via echo-antiecho strategy using both ^1H and ^{15}N gradients, as well as phase cycling. T_1/T_2 sequences were written to run in pseudo3d mode with ^1H and ^{15}N being the two time/frequency dimensions while the third dimension was a list of relaxation delays. The indirect time increment was interleaved with the relaxation delays; that is, for each indirect time point, data for all of the relaxation delays were acquired, subsequently incrementing the T_1 value.

For the T_1 and T_2 data, 32 transients were averaged for datasets consisting of 1,024 by 128 complex points using a recycle delay of 3 s. The relaxation delays for the T_1 ($1/R_1$) measurements were 0, 90, 200, 320, 460, 620, 820, 1,080, 1,450, 2,070, 3,000, and 5,000 ms. The relaxation delays for the T_2 ($1/R_2$) measurements were 0, 8, 16, 24, 32, 40, 48, 56, 64, 80, 96, 120, 160, and 248 ms. The NOE and no NOE experiments were run in an interleaved fashion with recycle delays of 5 s, 128 transients per increment, as 1,024 by 90 complex points in proton and nitrogen, respectively. NMR data were processed using NMRPipe (41), and analyzed using NMRView (42). The selection of ordered, nonexchanging resonances from the nSH2 domain, and the estimation and error analysis of rotational correlation times were done using DASHA (43). HYDRONMR (34) was used to calculate the expected rotational correlation times and relaxation rates for the individual and combined p85ni domains.

PI 3-Kinase Assays. Wild-type or mutant p110α, produced in Sf-9 cells, was incubated without or with wild-type or mutant p85ni, and PI 3-kinase activity were measured as described in ref. 33. Statistical significance was determined using ANOVA and the Tukey HSD test (at http://faculty.vassar.edu/lowry/VassarStats.html).

Transfections and Western Blot Analysis. HEK 293T cells were transiently transfected with myc-p110α and wild-type or mutant p85ni. Cells were starved overnight, stimulated with insulin for 5–30 min, lysed, and blotted for Akt, pS473-Akt, pT308-Akt, pS65–4EBP1, total, and pS389-S6K1 (Cell Signaling Technologies), and pT246-PRAS40 (Biosource). When indicated, cells were cotransfected with HA-S6K1 or HA-Akt, and phosphorylation was analyzed in anti-HA immunoprecipitates.

BaF3 Stable Cell Lines and Signaling. Wild-type or mutant p85ni and wild-type myc-p110α was stably transfected into IL-3-dependent mouse pre-B BaF3 cells using retrovirus produced using the pRetro-IRESdsRed vector (Clontech), or a variant expressing GFP. Cells were sorted by flow cytometry based on expression of dsRed and GFP, expanded and characterized for expression of proteins and signaling by Western blot.

PDGF-R Binding Assays. HEK293T cells were co-transfected with myc-p110α, wild-type or mutant HA-p85ni, and human PDGFβ receptor. Cells were stimulated without or with PDGF for 10 min, and anti-HA immunoprecipitates were blotted with anti-PDGF-R antibody.

Transformation Assays. NIH 3T3 cells were transiently transfected with myc-p110α and wild-type or mutant p85ni. Two days after transfection, the cells (2,500 cells/well) were plated in 1 mL of 0.3% top agar, on 1 mL of 0.6% bottom agar, in a six-well dish. Cell colonies were counted after 3 weeks.

Anti-PIP3 Staining. Cells were fixed and stained with anti-HA antibody (to detect transfected cells) and anti-PIP3 IgG (Echelon) as described in ref. 39. For fluorescence quantification, all digital images were imported in NIH image software and analyzed by using a previously described macro (45). This macro collects pixel intensities from the perimeter of the cell in a 0.22-m stepwise manner. The pixel intensities in the leading-edge compartment, defined as 0.66 m from the perimeter of the cells, were averaged and normalized to the edge intensity of nonstimulated cells.

ACKNOWLEDGMENTS. This work was supported by the Janey Fund and the National Institutes of Health Grants GM55692 (to J.M.B.), GM072085 (to M.E.G.), and GM075920 (to G.J.G.), the Albert Einstein Comprehensive Cancer Center Grant P30 CA013330, and Diabetes Training and Research Center Grant DK020541. J.M.B and M.E.G are members of the New York Structural Biology Center (NYSBC). The NYSBC is a Strategically Targeted Research Center supported by the New York State Office of Science, Technology, and Academic Research. NYSBC NMR resources are supported by the National Institutes of Health Grant P41 GM66354.

1. Engelman JA, Luo J, Cantley LC (2006) The evolution of phosphatidylinositol 3-kinases as regulators of growth and metabolism. *Nat Rev Genet* 7:606–619.
2. Auger KR, Serunian LA, Soltoff SP, Libby P, Cantley LC (1989) PDGF-dependent tyrosine phosphorylation stimulates production of novel polyphosphoinositides in intact cells. *Cell* 57:167–175.
3. Vanhaesebroeck B, et al. (2001) Synthesis and function of 3-phosphorylated inositol lipids. *Annu Rev Biochem* 70:535–602.
4. Kodaki T, et al. (1994) The activation of phosphatidylinositol 3-kinase by Ras. *Curr Biol* 4:798–806.
5. Yu J, et al. (1998) Regulation of the p85/p110 phosphatidylinositol 3′-kinase: Stabilization and inhibition of the p110-alpha catalytic subunit by the p85 regulatory subunit. *Mol Cell Biol* 18:1379–1387.
6. Wu H, Yan Y, Backer JM (2007) Regulation of class IA PI3Ks. *Biochem Soc Trans* 35:242–244.
7. Koyama S, et al. (1993) Structure of the PI3K SH3 domain and analysis of the SH3 family. *Cell* 72:945–952.
8. Liang J, Chen JK, Schreiber SL, Clardy J (1996) Crystal structure of P13K SH3 domain at 2.0 Å resolution. *J Mol Biol* 257:632–643.
9. Booker GW, et al. (1993) Solution structure and ligand-binding site of the SH3 domain of the p85α subunit of phosphatidylinositol 3-kinase. *Cell* 73:813–822.
10. Musacchio A, Cantley LC, Harrison SC (1996) Crystal structure of the breakpoint cluster region-homology domain from phosphoinositide 3-kinase p85 alpha subunit. *Proc Natl Acad Sci USA* 93:14373–14378.
11. Nolte RT, Eck MJ, Schlessinger J, Shoelson SE, Harrison SC (1996) Crystal structure of the PI 3-kinase p85 amino-terminal SH2 domain and its phosphopeptide complexes. *Nat Struct Biol* 3:364–374.
12. Siegal G, et al. (1998) Solution structure of the C-terminal SH2 domain of the p85α regulatory subunit of phosphoinositide 3-kinase. *J Mol Biol* 276:461–478.
13. Hoedemaeker FJ, Siegal G, Roe SM, Driscoll PC, Abrahams JP (1999) Crystal structure of the C-terminal SH2 domain of the p85α regulatory subunit of phosphoinositide 3-kinase: An SH2 domain mimicking its own substrate. *J Mol Biol* 292(4):763–770.
14. Fu Z, Aronoff-Spencer E, Backer JM, Gerfen GJ (2003) The structure of the inter-SH2 domain of class IA phosphoinositide 3-kinase determined by site-directed spin labeling EPR and homology modeling. *Proc Natl Acad Sci USA* 100:3275–3280.
15. Miled N, et al. (2007) Mechanism of two classes of cancer mutations in the phosphoinositide 3-kinase catalytic subunit. *Science* 317:239–242.
16. Huang CH, et al. (2007) The structure of a human p110α/p85α complex elucidates the effects of oncogenic PI3Kα mutations. *Science* 318:1744–1748.
17. Walker EH, Perisic O, Ried C, Stephens L, Williams RL (1999) Structural insights into phosphoinositide 3-kinase catalysis and signalling. *Nature* 402:313–320.
18. Klippel A, Escobedo JA, Hu Q, Williams LT (1993) A region of the 85-kilodalton (kDa) subunit of phosphatidylinositol 3-kinase binds the 110-kDa catalytic subunit in vivo. *Mol Cell Biol* 13:5560–5566.
19. Hu P, Mondino A, Skolnik EY, Schlessinger J (1993) Cloning of a novel, ubiquitously expressed human phosphatidylinositol 3-kinase and identification of its binding site on p85. *Mol Cell Biol* 13:7677–7688.
20. Holt KH, Olson AL, Moye-Rowley WS, Pessin JE (1994) Phosphatidylinositol 3-kinase activation is mediated by high-affinity interactions between distinct domains within the p110 and p85 subunits. *Mol Cell Biol* 14:42–49.
21. Backer JM ,et al. (1992) The phosphatidylinositol 3′-kinase is activated by association with IRS-1 during insulin stimulation. *EMBO J* 11:3469–3479.
22. Carpenter CL, et al. (1993) Phosphoinositide 3-kinase is activated by phosphopeptides that bind to the SH2 domains of the 85-kDa subunit. *J Biol Chem* 268:9478–9483.
23. Yu JH, Wjasow C, Backer JM (1998) Regulation of the p85/p110α phosphatidylinositol 3′-kinase - Distinct roles for the N-terminal and C-terminal SH2 domains. *J Biol Chem* 273:30199–30203.
24. O'Brien R, et al. (2000) Alternative modes of binding of proteins with tandem SH2 domains. *Protein Sci* 9:570–579.
25. Fu Z, Aronoff-Spencer E, Wu H, Gerfen GJ, Backer JM (2004) The iSH2 domain of PI 3-kinase is a rigid tether for p110 and not a conformational switch. *Arch Biochem Biophys* 432:244–251.
26. Samuels Y, et al. (2004) High frequency of mutations of the PIK3CA gene in human cancers. *Science* 304:554.
27. Zhao L, Vogt PK (2008) Helical domain and kinase domain mutations in p110α of phosphatidylinositol 3-kinase induce gain of function by different mechanisms. *Proc Natl Acad Sci USA* 105:2652–2657.
28. Jimenez C, et al. (1998) Identification and characterization of a new oncogene derived from the regulatory subunit of phosphoinositide 3-kinase. *EMBO J* 17:743–753.
29. Jucker M, et al. (2002) Expression of a mutated form of the p85α regulatory subunit of phosphatidylinositol 3-kinase in a Hodgkin's lymphoma-derived cell line (CO). *Leukemia* 16:894–901.
30. Philp AJ, et al. (2001) The phosphatidylinositol 3′-kinase p85α gene is an oncogene in human ovarian and colon tumors. *Cancer Res* 61:7426–7429.
31. Parsons DW, et al. (2008) An integrated genomic analysis of human glioblastoma multiforme. *Science* 321:1807–1812.
32. Network CGAR (2008) Comprehensive genomic characterization defines human glioblastoma genes and core pathways. *Nature* 455:1061–1068.
33. Shekar SC, et al. (2005) Mechanism of constitutive PI 3-kinase activation by oncogenic mutants of the p85 regulatory subunit. *J Biol Chem* 280:27850–27855.
34. Bernado P, Garcia de la Torre J, Pons M (2002) Interpretation of 15N NMR relaxation data of globular proteins using hydrodynamic calculations with HYDRONMR. *J Biomol NMR* 23:139–150.
35. Fushman D, Xu R, Cowburn D (1999) Direct determination of changes of interdomain orientation on ligation: Use of the orientational dependence of 15N NMR relaxation in Abl SH(32). *Biochemistry* 38:10225–10230.
36. Farrow NA, et al. (1994) Backbone dynamics of a free and phosphopeptide-complexed Src homology 2 domain studied by 15N NMR relaxation. *Biochemistry* 33:5984–6003.
37. Zhang W, Smithgall TE, Gmeiner WH (1998) Self-association and backbone dynamics of the hck SH2 domain in the free and phosphopeptide-complexed forms. *Biochemistry* 37:7119–7126.
38. Yip SC, et al. (2008) Quantification of PtdIns(3,4,5)P(3) dynamics in EGF-stimulated carcinoma cells: A comparison of PH-domain-mediated methods with immunological methods. *Biochem J* 411:441–448.
39. Gymnopoulos M, Elsliger MA, Vogt PK (2007) Rare cancer-specific mutations in PIK3CA show gain of function. *Proc Natl Acad Sci USA* 104:5569–5574.
40. Zhu G, Xia Y, Nicholson LK, Sze KH (2000) Protein dynamics measurements by TROSY-based NMR experiments. *J Magn Reson* 143:423–426.
41. Delaglio F, et al. (1995) NMRPipe: A multidimensional spectral processing system based on UNIX pipes. *J Biomol NMR* 6:277–293.
42. Johnson BA (2004) Using NMRView to visualize and analyze the NMR spectra of macromolecules. *Methods Mol Biol* 278:313–352.
43. Orekhov VY, Nolde DE, Golovanov AP, Korzhnev DM, Arseniev AS (1995) Processing of heteronuclear NMR relaxation data with the new software DASHA. *Appl Magn Reson* 9:581–588.
44. Yip SC, et al. (2007) The distinct roles of Ras and Rac in PI 3-kinase-dependent protrusion during EGF-stimulated cell migration. *J Cell Sci* 120:3138–3146.
45. DesMarais V, Ichetovkin I, Condeelis J, Hitchcock-Degregori SE (2002) Spatial regulation of actin dynamics: A tropomyosin-free, actin-rich compartment at the leading edge. *J Cell Sci* 115:4659–4660.